Title

Kinetics of cortical bone demineralization: Controlled demineralization—a new method for modifying cortical bone allografts

Journal

Journal of Biomedical Materials Research, 31(3)

ISSN

0021-9304

Authors

Lewandrowski, Kai-Uwe
Venugopalan, Vasan
Tomford, William W
et al.

Publication Date

1996-07-01

DOI

10.1002/(sici)1097-4636(199607)31:3<365::aid-jbm10>3.0.co;2-i

Kinetics of cortical bone demineralization: Controlled demineralization—a new method for modifying cortical bone allografts

Kai-Uwe Lewandrowski,[1] Vasan Venugopalan,[2] William W. Tomford,[1] Kevin T. Schomacker,[2] Henry J. Mankin,[1] and Thomas F. Deutsch[2,*]

[1]Orthopaedic Research Laboratory, and [2]Wellman Laboratories of Photomedicine, Massachusetts General Hospital, 50 Blossom Street, Boston, Massachusetts 02114

We investigated the kinetics of hydrochloric acid demineralization of human cortical bone with the objective of developing a method of controlled demineralization for structural bone allografts. It is known that the demineralization of cortical bone is a diffusion rate limited process with a sharp advancing reaction front. The demineralization kinetics of human cortical bone, described as the advance of the reaction front versus immersion time, were determined by measuring extraction of bone mineral in both planar and cylindrical geometries. Mathematical models based on diffusional mass transfer were developed to predict this process. The experimental data fit well with the behavior predicted by the model. The model for planar geometry is applicable to controlled demineralization of cortical bone allografts of irregular shapes such as cortical struts. The model for cylindrical geometry is appropriate when curved surfaces are involved such as in diaphyseal bone allografts. This method of demineralization has direct application to clinical modification of cortical bone allografts to potentially enhance their osteoinductive properties. © 1996 John Wiley & Sons, Inc.

INTRODUCTION

Cortical bone allografts are frequently used in orthopedic surgery to reconstruct extensive skeletal defects encountered in the treatment of bone tumors and osteolysis in failed joint replacements.[1-3] Although frequently successful, incorporation of these types of grafts is slow and unpredictable, resulting in nonunion and fatigue fractures.[2-6] We studied the demineralization of cortical bone in an attempt to provide a method which would improve the incorporation of these types of bone grafts.

The osteoinductive potential of demineralized cortical bone has been demonstrated in numerous experimental and clinical studies.[7-13] The osteoinductive effect of demineralized cortical bone relies on matrix factors such as the bone morphogenetic proteins (BMPs) of the TGF-beta gene family and other noncollagenous proteins. These growth factors appear to stimulate the transformation of non-osseous connective tissue cells into osteogenic and chondrogenic cells, regulate the resorption of cortical bone, and lead to formation of new bone.[14-18]

*To whom correspondence should be addressed; e-mail: deutsch@helix.mgh.harvard.edu.

However, the use of fully demineralized cortical bone allografts for reconstruction of long bones is not feasible in clinical practice because these grafts are not sufficiently stable to withstand normal skeletal forces. Partial demineralization of cortical bone allografts may provide a means of enhancing their osteoinductive properties while retaining their biomechanical strength. However, this requires the ability to precisely control the demineralization process, a method that is absent from previous studies.[7,19]

The process of bone demineralization is used extensively in the preparation of bone specimens for histological study and is well known to result in removal of calcium from bone. A variety of strong and weak acids, as well as acidic buffers, have been used for rapid decalcification.[20] In the case of acid demineralization using HCl, the major inorganic constituents in bone including hydroxyapatite, tricalcium phosphate, and calcium carbonate react to form calcium chloride.[21,22] A number of authors have approached the problem of understanding the process of demineralization or decalcification.[20-24] In particular, Makarewicz et al.,[21,22] whose interest in bone demineralization stemmed from its importance in the production of photographic gelatin, have demonstrated that the kinetics of demineralization were limited by the rate of diffusion of acid

Journal of Biomedical Materials Research, Vol. 31, 365–372 (1996)

CCC 0021-9304/96/030365-08

into bone tissue, with the dissolution of bone calcium phosphate salts being instantaneous by comparison. The demineralization kinetics were described by a "classic shrinking-core reaction model."[21,22,25] This work demonstrated that acid decalcification of bone was described by a diffusion model which was characterized by a moving reaction front.

The fact that the demineralization process is diffusion-limited means that the kinetics of the demineralization of any geometry of bone can be predicted, providing the diffusion equation can be solved for that geometry, and that the diffusivity of acid into bone is known. This in turn allows the formulation of models applicable to the specific geometric and tissue characteristics of human cortical bone allografts.

Therefore we studied the kinetics of hydrochloric acid demineralization of cortical bone in order to obtain the diffusivity for HCl into human cortical bone, and to verify the applicability of the diffusion model for both planar and cylindrical geometries. The ultimate objective of these studies was to quantify the technique for producing partially demineralized cortical bone allografts that would be rapidly incorporated, while allowing stable reconstruction.

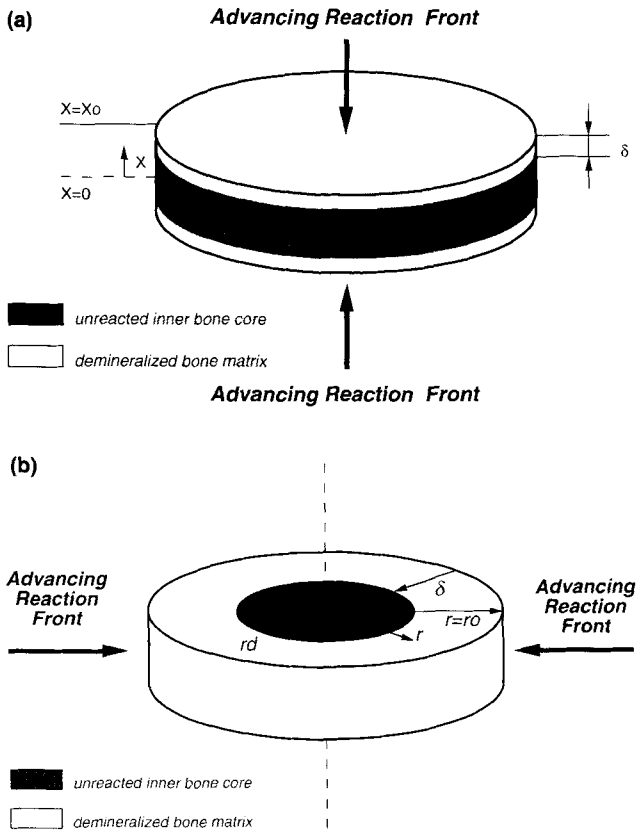

Figure 1. (a) Planar model. Peripheral rim of the bone disc is epon coated. Demineralization proceeds from top and bottom surfaces: x_0 = distance from outer surface to the center line; x = any given position between center line and outer surface, i.e., the distance from the center line to the reaction front, δ = penetration depth. (b) Cylindrical model. Top and bottom surface of the bone is disc epon coated. Demineralization proceeds from peripheral rim: r_0 = the initial radius; r = any radial position, i.e., the radial position of the reaction front; r_d = radius of the remaining inner undemineralized bone core; δ = penetration depth ($\delta = r_0 - r_d$).

MATERIALS AND METHODS

The experimental bones used in this study were 7 human tibias. They were obtained from 7 young healthy white males with ages ranging from 25 to 39 years, and an average age of 32 years. The bones were provided by a bone bank which had to discard them due to bacterial contamination.

Demineralization kinetics studies

To investigate the demineralization kinetics of cortical bone, diaphyses of human tibias were cut into uniform discs of 5 mm diameter and 2 mm thickness. These discs were used to create two geometrical models by coating various surfaces of the discs with an acid-resistant epon layer. A planar geometry model was created by coating the circumference of a disc [Fig. 1(a)], and a cylindrical geometry model was obtained by coating the top and bottom surface of a disc [Fig. 1(b)]. This allowed the demineralization process to occur either from the top and bottom surface (planar geometry) or from the circumference (cylindrical geometry). Demineralization of these discs was performed by immersion in hydrochloric acid at concentrations of 0.5N (1.875% w/v), 1N (3.65% w/v), and 2N (7.3% w/v) for various times. An excess of acid volume was employed to avoid depletion of the acid concentration in the bath, and the acid bath was agitated to provide uniform concentration. Demineralization of the bone discs was terminated by multiple washings in 4°C distilled water until pH 7 was reached. Bone discs were then dehydrated by immersion in 98% ethyl alcohol for 1 h, anhydrous ether extraction for 1 h, and air drying for 1 h.

Using a Mettler AE 163 precision balance, the time course for bone mineral extraction for immersion time in HCl was determined by measuring the dry weight of the discs before and after demineralization at different immersion times. Three randomly selected bone disc specimens were included for each demineralization time point at a specific acid concentration. For the cylindrical geometry 8 time points were studied, corresponding to 24 bone disc specimens for each concentration, or a total of 72 specimens in all. For the planar geometry only 7 time points were evaluated, resulting in 21 specimens for each concentration, or a total of 63 specimens in all. The average of the normalized weight

loss of bone discs [Eqs. (1) and (2) described below] was used to quantify the kinetics of the demineralization process.

RESULTS

Demineralization kinetics studies and analytical modeling

The penetration depth of the demineralization process was obtained from the measured weight loss. This was done by normalizing the weight loss for a particular immersion time to the weight loss corresponding to total demineralization, and setting that equal to volume of the demineralized region normalized to the initial volume. For the planar geometry this yields the following expression for the penetration depth (δ) at a particular immersion time t:

$$\delta(t) = \frac{T}{2}\left[1 - \frac{W(t) - W_\infty}{W_0 - W_\infty}\right], \quad (1)$$

where W_0 is the initial weight prior to demineralization, $W(t)$ the weight after demineralization, and W_∞ the average weight of bone specimens at total demineralization (infinite immersion time). The distance from the top and bottom surfaces to the center line of the bone discs [Fig. 1(a)], where the two reaction fronts meet at complete demineralization, is half the thickness of the bone disc (T/2 = 1000 μm).

In analogy, the penetration depth (δ) of the demineralization process of cylindrical geometries at a particular immersion time t, was calculated as:

$$\delta(t) = r_0\left[1 - \sqrt{\frac{W(t) - W_\infty}{W_0 - W_\infty}}\right], \quad (2)$$

where r_0 is the initial radius. In both geometrical models, the data is normalized by the initial weight of the bone discs [Eqs. (1) and (2)], and are presented as single data points. Figs. 2 and 3 show the respective kinetic data for planar and cylindrical geometry which are plotted as the remaining core thickness ($x_0 - \delta$) or radius ($r_0 - \delta$) (mm) versus immersion time t (h) for the above-noted acid concentrations. The average bone mineral content (BMC) of human cortical bone determined from the residual weight of the bone discs upon complete demineralization was found to be 67 ± 2%.

For modeling purposes we analyzed the kinetics of the demineralization experiments using the diffusion equation with an advancing reaction front in both planar and cylindrical geometry. The analysis served to test the diffusion formalism to accurately predict the demineralization process of human cortical bone.

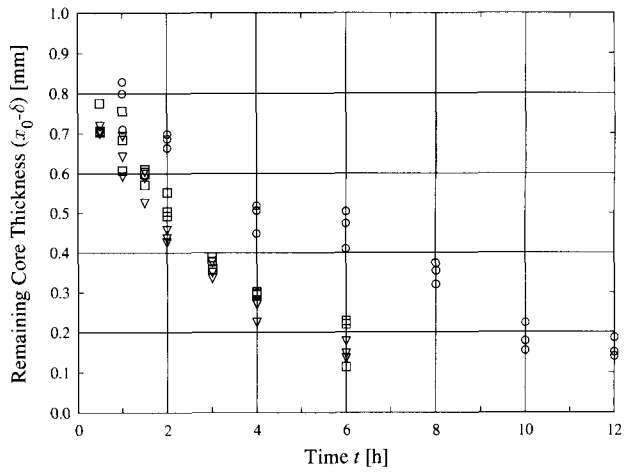

Figure 2. Remaining core thickness ($x_0 - \delta$) (mm) vs. immersion t (h) for human cortical bone for acid concentrations of 0.5N (○), 1N (□), and 2N HCl (▽) in planar geometry. Raw data fit to the model presented in Equation (3).

As described previously,[21–23,25] the assumptions of this model are: (1) the demineralization of cortical bone with hydrochloric acid is a diffusion process in a fluid–solid system with a sharp advancing reaction front, and can be described with Fick's Law; (2) the acid concentration gradient between undemineralized bone and bath is the driving force for the mass flux of acid into bone; (3) the acid concentration at the exposed outer surfaces of the bone specimens equals the bath concentration; (4) acid diffuses into bone, and reacts instantaneously with the bone mineral upon arrival at the reaction front. Thus the process can be considered to be diffusion-rate–limited and the concentration profile of acid within the demineralized bone matrix is quasi static.

The details of the analytical modeling and the solution of the diffusion equation in both geometries are

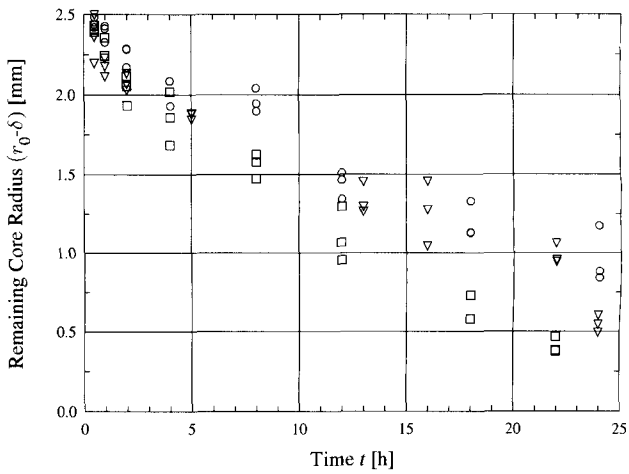

Figure 3. Remaining core radius ($r_0 - \delta$) (mm) vs. immersion t (h) for human cortical bone for acid concentrations of 0.5N (○), 1N (□), and 2N HCl (▽) in cylindrical geometry. Raw data fit to the model presented in Equation (4).

given in the APPENDIX (A refers to equations presented in the appendix). The analytical models which allow prediction of demineralization depth as a function of immersion time and acid concentration are briefly summarized here.

For planar geometry the depth of penetration of the demineralization process as a function of immersion time t in acid, $\delta(t)$ (cm) is given by:

$$\delta(t) = \sqrt{\frac{2DC_0t}{10^3\lambda}}. \quad (3)$$

where D is the effective mass diffusivity of HCl into the bone (cm^2/s), C_0 is the acid concentration (mol L), t the immersion time in the HCl acid bath (s), and λ the moles of acid necessary to demineralize 1 cm^3 of cortical bone completely (mol/cm^3). The 10^3 factor is used to convert cm^3 to liters.

Although the time dependence of the demineralization depth can also be expressed analytically in cylindrical geometry, it no longer has the simple square root of immersion time dependence found in planar geometry. The time necessary to achieve a radial penetration depth of the demineralization process $\delta(t)$ with $\delta(t) = r_0 - r_d(t)$ is given by:

$$t(\delta) = \frac{10^3\lambda r_0^2}{4C_0D}\left[2\frac{(r_0-\delta)^2}{r_0^2}\ln\left(\frac{r_0-\delta}{r_0}\right) - \frac{(r_0-\delta)^2}{r_0^2} + 1\right], \quad (4)$$

where r_0 is the initial radius of a cylindrical bone and $r_d(t)$ the radial position of the demineralization front measured from the center line at time t [Fig. 1(b)]. Note that the immersion time in hydrochloric acid required to obtain a certain demineralization depth depends on the initial radius of a cylindrical bone. The solution presented in Equation (4) is therefore normalized for this dependence.

Fit of experimental data to analytical models

In order to fit the experimental data to the analytical models, values of the effective mass diffusivities D at different acid concentrations and the value of λ as the amount of HCl required for complete demineralization of a specific volume of human cortical bone were determined. The value of λ was determined by titration in HCl dilution series using bone discs of planar geometry. Titration experiments were carried out in triplicate and determined λ to be 0.0144 mol/cm^3. The effective mass diffusivities D of HCl at each normality in human cortical bone were determined using each δ,t-pair and Equation (3) for planar geometry and each δ,t-pair and Equation (4) for cylindrical geometry, respectively. Student's t test was employed to test for significance in the data comparing planar to cylindrical geometries. The mean values for D, the p-values of the t test, and the maximum immersion time in HCl at each concentration for the two geometrical models are presented in Table I.

Kinetic data in planar and cylindrical geometry, when plotted as reduction of the dimensionless bone disc core thickness x^* with $x^* = x/x_0$ for planar geometry or as the reduction of the dimensionless bone disc radius r^* with $r^* = r_d/r_0$ for cylindrical geometry versus the dimensionless immersion time t^* with $t^* = Dt/x_0^2$ for planar and $t^* = Dt/r_0^2$ for cylindrical geometry on a log–log scale, fit well with the time dependencies predicted by Equations (3) and (4) (Figs. 4 and 5). Linear regression yielded regression coefficients of $0.968 < R^2 < 0.999$ for experimental data of planar geometry to the $\sqrt{t}$ dependence predicted by Equation (3).

The mathematical models describing the demineralization kinetics of cortical bone in planar [Eq. (3)] and cylindrical geometry [Eq. (4)] were used to generate ready-to-use look-up tables which allow determination of the immersion time in HCl necessary to obtain a certain penetration depth of the demineralization process (Tables II and III).

DISCUSSION

This study shows that hydrochloric acid demineralization of human cortical bone can be described with the theory of the shrinking core used for diffusion-limited processes in fluid–solid systems.[25] The shrinkage of the inner unreacted core is a function of the immersion time in acid. Cortical bone demineralization results in a sharp advancing reaction front that sepa-

TABLE I
Effective Mass Diffusivity, D, of HCl in Demineralized Bone Matrix (DBM) of Human Cortical Bone

C_{HCl} (N)	D of DBM of Human Cortical Bone Determined in Planar Geometry (10^{-6}) cm^2/s)	D of DBM of Human Cortical Bone Determined in Cylindrical Geometry [10^{-6} cm^2/s]	p-Values for D Obtained From Planar and Cylindrical Geometry	Maximum Immersion time t (h) for Bone Disc of Planar Geometry	Maximum Immersion time t (h) for Bone Disc of Cylindrical Geometry
0.5	2.31 ± 0.39	2.69 ± 0.52	0.180	17.3	46.5
1	2.35 ± 0.39	2.50 ± 0.29	0.038	8.5	25.0
2	1.33 ± 0.20	0.92 ± 0.15	1.7×10^{-7}	7.5	34.0

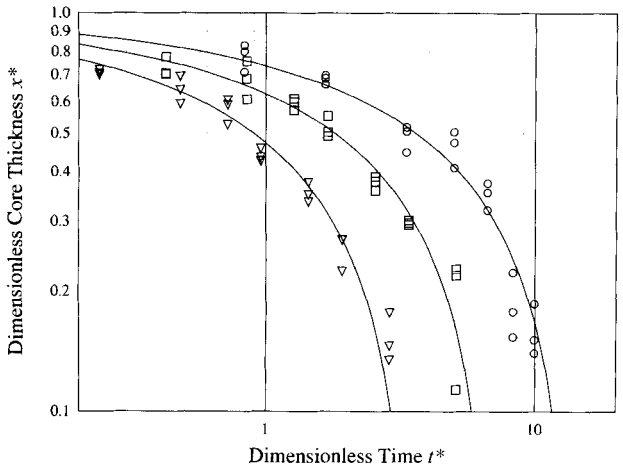

Figure 4. Demineralization depth in planar geometry plotted on a log–log scale as bone disc core thickness $x^* = x/x_0$ vs. the dimensionless immersion time $t^* = Dt/x_0^2$ for HCl concentrations of 0.5*N* (○), 1*N* (□), and 2*N* (▽). Data fit the $t^{1/2}$-dependence given in Equation (3) using values for the effective mass diffusivities *D* calculated from data in planar geometry and Equation (3).

rates the demineralized bone matrix from the remaining inner cortical bone core. As shown by the data, the position of the reaction front can be accurately modeled for both planar and cylindrical geometry.

The kinetic data in planar coordinates show that the penetration depth of the demineralization process increases linearly with the square root of the immersion time in hydrochloric acid. In cylindrical geometry the kinetics is more complex due to the continuous change of curvature of the remaining inner cortical bone core. However, the demineralization process is insensitive

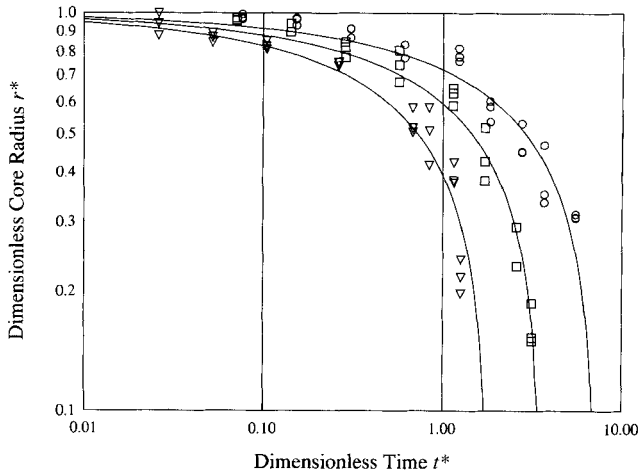

Figure 5. Demineralization depth in cylindrical geometry plotted on a log–log scale as dimensionless bone disc core radius $r^* = r_d/r_0$ versus the dimensionless immersion time $t^* = Dt/r_0^2$ for HCl concentrations of 0.5*N* (○), 1*N* (□), and 2*N* (▽). Data fit the time dependence predicted by Equation (4) using values for the effective mass diffusivities *D* calculated from data in cylindrical geometry and Equation (4).

TABLE II
Demineralization Kinetics of Human Cortical Bone in Planar Geometry-Penetration Depth vs. Immersion Time in HCl at Various Concentrations

Penetration Depth (mm)	Immersion Time in 0.5N HCl (h:min)	Immersion Time in 1*N* HCl (h:min)	Immersion Time in 2*N* HCl (h:min)
0	0	0	0
0.1	00:10	00:05	00:05
0.2	00:41	00:21	00:18
0.3	01:33	00:46	00:40
0.4	02:46	01:22	01:12
0.5	04:19	02:08	01:52
0.6	06:13	03:04	02:42
0.7	08:28	04:10	03:40
0.8	11:05	05:27	04:49
0.9	14:01	06:53	06:05
1.0	17:19	08:31	07:31
1.1	20:57	10:18	09:05
1.2	24:56	12:16	10:49
1.3	29:16	14:23	12:42
1.4	33:56	16:41	14:44
1.5	38:58	19:09	16:55
1.6	44:19	21:48	19:14
1.7	50:02	24:36	21:43
1.8	56:06	27:34	24:22
1.9	62:31	30:43	27:08
2.0	69:16	34:02	30:04
2.1	76:22	37:32	33:09
2.2	83:48	41:11	36:23
2.3	91:36	45:01	39:46
2.4	99:44	49:01	43:18
2.5	108:13	53:11	46:59
2.6	117:03	57:32	50:49
2.7	126:14	62:02	54:48
2.8	135:45	66:43	58:56
2.9	145:37	71:34	63:14
3.0	155:50	76:36	67:40

to acid concentration higher than 1*N*. This is shown in Table I where the diffusivity of the demineralized bone matrix is reduced for increasing acid concentrations. This decrease in the diffusivity results in a reduction of the speed at which the demineralization proceeds at higher acid concentrations. This effect is seen in the raw data (Figs. 2 and 3), where the difference in slope between the curves for 1*N* and 2*N* is not as large as that between the 0.5*N* and 1.0*N* curves.

The reduction in diffusivity of demineralized cortical bone may be related to an alteration of collagen and other bone matrix proteins, which progresses with increasing immersion times and acid concentration. The protein degradation, as measured by nitrogen content of the acid liquor, has been found to be nearly constant for acid concentrations up to 4% w/v (1.1*N*) HCl, but increases threefold when the concentration is increased to 8% w/v (2.2*N*).[21-23] This results in an interdependence between the effective mass diffusivity *D* and the acid concentration C_0. The reduced values for *D* at higher acid concentrations corroborate this hypothesis

TABLE III
Immersion Time of Human Cortical Bone in 0.5*N* HCl for Cylindrical Geometry-Penetration Depth vs. Initial Outer Radius

Demineralization Depth (mm)	Initial Outer Radius of a Cylindrical Bone Graft (mm)										
	5	6	7	8	9	10	12	14	16	18	20
0.1	00:09	00:09	00:09	00:09	00:09	00:09	00:09	00:09	00:09	00:09	00:29
0.2	00:35	00:35	00:35	00:35	00:35	00:35	00:35	00:35	00:35	00:35	00:35
0.3	01:19	01:19	01:19	01:19	01:19	01:19	01:20	01:20	01:20	01:20	01:20
0.4	02:19	02:20	02:20	02:20	02:20	02:21	02:21	02:22	02:22	02:22	02:22
0.5	03:35	03:37	03:38	03:38	03:39	03:39	03:40	03:40	03:41	03:41	03:41
0.6	05:08	05:10	05:12	05:13	05:14	05:14	05:16	05:17	05:17	05:17	05:18
0.7	06:56	06:59	07:02	07:04	07:05	07:07	07:08	07:10	07:11	07:11	07:12
0.8	08:59	09:05	09:08	09:11	09:14	09:16	09:18	09:20	09:22	09:22	09:23
0.9	11:17	11:25	11:31	11:35	11:38	11:40	11:44	11:47	11:49	11:50	11:52
1.0	13:49	14:01	14:08	14:14	14:18	14:22	14:27	14:31	14:34	14:35	14:37
1.1	16:35	16:50	17:01	17:08	17:14	17:19	17:26	17:31	17:34	17:37	17:40
1.2	19:35	19:55	20:08	20:18	20:26	20:32	20:41	20:47	20:52	20:56	20:59
1.3	22:47	23:13	23:30	23:43	23:52	24:00	24:12	24:20	24:26	24:31	24:35
1.4	26:13	26:44	27:06	27:22	27:34	27:44	27:59	28:09	28:17	28:22	28:27
1.5	29:50	30:28	30:56	31:16	31:31	31:43	32:01	32:14	32:23	32:31	32:36
1.6	33:38	34:26	34:59	35:23	35:42	35:57	36:19	36:34	36:46	36:55	37:02
1.7	37:37	38:35	39:16	39:45	40:08	40:26	40:52	41:11	41:25	41:35	41:44
1.8	41:47	42:57	43:45	44:20	44:47	45:09	45:40	46:02	46:19	46:32	46:42
1.9	46:07	47:30	38:27	49:09	49:41	50:07	50:44	51:10	51:29	51:44	51:56
2.0	50:36	52:14	54:22	54:11	54:48	55:18	56:02	56:32	56:55	57:13	57:27
2.1	55:13	57:08	58:28	59:25	60:09	60:43	61:34	62:10	62:37	62:57	63:13
2.2	59:59	62:13	63:45	64:52	65:43	66:22	67:21	68:02	68:33	68:56	69:16
2.3	64:53	67:28	69:14	70:31	71:29	72:15	73:22	74:10	74:45	75:12	75:34
2.4	69:53	72:52	74:53	76:21	77:28	78:20	79:38	80:32	81:12	81:43	82:07
2.5	74:59	78:24	80:43	82:23	83:40	84:39	86:07	87:08	87:53	88:29	88:56
2.6	80:11	84:05	86:43	88:37	90:03	91:10	92:50	93:59	94:50	95:29	96:01
2.7	85:28	89:53	92:52	95:01	96:38	97:54	99:46	101:04	102:02	102:46	103:21
2.8	90:48	95:49	99:10	101:35	103:25	104:50	106:56	108:59	109:28	110:17	110:56
2.9	96:12	101:50	105:37	108:20	110:22	111:58	114:19	115:56	117:08	118:03	118:47
3.0	101:38	107:59	112:13	115:14	117:31	119:18	121:54	123:43	125:02	126:04	126:52

(Table I). In addition we found that the *D* values obtained in planar and cylindrical geometry are significantly different for 1*N* and 2*N* HCl (Table I). The longer immersion time in cylindrical geometry for complete demineralization, as shown in Table I, may have led to more extensive degradation of the bone matrix thus reducing its diffusivity.

Although cortical bone specimens from selected young healthy donors were used in this analysis, the measured values for the diffusivity D for human demineralized bone matrix appear generally applicable to cortical bone from different donors. As noted, the measured values for D in cattle bone are less than 25% higher than those for human cortical bone in the same geometry, suggesting that variations between human samples should be even less.[21,22] In addition, as the depth of demineralization depends on the square root of D [Eq. (3)], the sensitivity of demineralization depth to variations in D is weak.

We investigated the kinetics of HCl demineralization of human cortical bone in two geometries frequently encountered in clinical bone allografts. The planar model can be considered the best approximation for bone grafts with irregular planar shapes such as cortical struts. The cylindrical model is applicable for grafts with curved surfaces such as long diaphyseal bone grafts.

The results of the model in both planar and cylindrical geometries allow prediction of the demineralization of cortical bone allografts of most sizes and shapes. They provide the theoretical basis for modifying clinically used cortical bone allografts to grafts which have a highly osteoinductive surface layer. This new method of controlled demineralization should provide a means to produce cortical bone allografts which are rapidly incorporated and yet retain the biomechanical strength required for stable reconstruction.

APPENDIX

Modeling for planar geometries

To model the demineralization kinetics in planar geometry [Fig. 1(a)], the top and bottom surface of the

bone discs can be considered as semi-infinite sheets. Consistent with the theoretical assumption of a quasi-steady state process Fick's Law is used in a one-dimensional cartesian coordinate system:

$$\frac{\partial^2 m}{\partial x^2} = 0, \tag{A1}$$

where m is the mass concentration of hydrochloric acid (mass of acid/mass of solution) and x the axial position in the sample measured from the center line [Fig. 1(a)]. The boundary conditions are given with an acid concentration of zero at the interface between demineralized bone matrix and cortical bone, $m(x = x_0 - \delta) = 0$, and an acid concentration at the outer surface of the bone disc equal to the bath concentration, $m(x = x_0) = m_0$. Integrating Equation (A1) and solving for the boundary conditions yields:

$$m(x,t) = m_0\left[1 - \frac{x}{\delta(t)}\right], \tag{A2}$$

where m_0 is the mass concentration of HCl in the bath, m is the mass concentration of HCl at any given position x in the sample and $\delta(t)$ the depth of demineralization at time t. To determine the penetration depth $\delta(t)$ mass conservation at the reaction front $x = \delta$ is enforced as follows:

$$M\lambda\frac{\partial\delta}{\partial t} = -\rho D\left.\frac{\partial m}{\partial x}\right|_{x=\delta}, \tag{A3}$$

where M is the molecular weight of HCl (g/mol), λ the moles of acid necessary to demineralize 1 cm^3 of cortical bone (mol/cm^3), D the mass diffusivity of HCl into the bone (cm^2/s) and the density of the acid solution (g/cm^3). Equation (A3) relates the mass flux of acid into cortical bone with the rate at which the demineralization front proceeds. Taking the derivative of Equation (A2) and substituting into Equation (A3) yields upon integration:

$$\delta(t) = \sqrt{\frac{2\rho D m_0 t}{M\lambda}}. \tag{A4}$$

The acid bath concentration C_0 in mol/L is related to the mass concentration of HCl m_0 as

$$C_0 = \frac{\rho m_0 10^3}{M}. \tag{A5}$$

Substituting C_0 for the mass concentration of the acid bath m_0 yields the relation expressed in Equation (3) as mentioned above. Equation (A4) may be expressed as:

$$\delta = k\sqrt{t}, \tag{A6}$$

where $k = (2\rho D m_0/M\lambda)^{1/2}$ is the slope of the linear function $\delta(\sqrt{t})$. Using the value of k defined by the data and λ determined by titration the effective mass diffusivity D of HCl into bone can be calculated with:

$$D = \frac{k^2\lambda}{2C_0}. \tag{A7}$$

Modeling for cylindrical geometries

In cylindrical coordinates Fick's Law is expressed as:

$$\frac{1}{r}\frac{\partial}{\partial r}\left(r\frac{\partial m}{\partial r}\right) = 0, \tag{A8}$$

where r is the radius of a cylindrical bone. As such the penetration depth as a function of immersion time is dependent on the initial radius r_0. Therefore it is advantageous to normalize for r_0, and to perform the analysis with dimensionless variables. Equation (A8) may be rewritten as:

$$\frac{1}{r^*}\frac{\partial}{\partial r^*}\left(r^*\frac{\partial m^*}{\partial r^*}\right) = 0, \tag{A9}$$

where $m^*(r) = m(r)/m_0$, $r^* = r_d/r_0$, $r_d^* = r_d/r_0$ (Fig. 2). The boundary conditions become $m^*(r^* = 1) = 1$ and $m^*(r^* = r_d^*) = 0$. Integrating Fick's Law for cylindrical geometry [Eq. (A9)], and applying the boundary conditions yields:

$$m^*(r^*) = 1 - \left(\frac{\ln r^*}{\ln r_d^*}\right). \tag{A10}$$

To obtain a relation for the penetration depth of the demineralization process δ as a function of the immersion time t, mass conservation at the reaction front is enforced which gives:

$$M\lambda\frac{\partial r_d}{\partial t} = -\rho D\left.\frac{\partial m}{\partial r}\right|_{r=r_d}. \tag{A11}$$

Rewriting Equation (A10) using the dimensionless variables $m^* = m/m_0$, $r^* = r_d/r_0$, $t^* = Dt/r_0^2$ and $\eta = \rho m_0/M\lambda$, a parameter related to the demineralization strength of the acid employed, yields:

$$\frac{\partial r_d^*}{\partial t^*} = -\eta\left.\frac{\partial m^*}{\partial r^*}\right|_{r^*=r_d^*}. \tag{A12}$$

Taking the derivative of m^* in Equation (A10) and substituting into Equation (A12) yields upon integration:

$$2r_d^{*2}\ln r_d^* - r_d^{*2} + 1 = 4\eta t^*. \tag{A13}$$

Equation (A13) gives the radial position of the demineralization front r_d in cylindrical geometry measured from the center line. In order to obtain a relation that determines the immersion time t necessary to demineralize to a certain penetration depth δ with $\delta(t) = r_0 - r_d(t)$, Equation (A13) can be rewritten by substituting

C_0 for the mass concentration of the acid bath m_0 with Equation (A5), and solved for t as mentioned above in Equation (4).

This work was supported by NIH Grant AR-21896, the Medical Free Electron Laser Program under Office of Naval Research contract N00014-94-I-0927 and by Doe Grant # DE-FG02-91 ER61228.

References

1. F. Enneking and E. R. Mindell, "Observations on massive retrieved human allografts," *J. Bone Joint Surg.*, **73A,** 1123–1142 (1991).
2. H. J. Mankin, D. S. Springfield, M. C. Gebhardt, and W. W. Tomford, "Current status of allografting for bone tumors," *Orthopedics*, **15,** 1147–1154 (1992).
3. H. J. Mankin, S. Doppelt, and W. Tomford, "Clinical experience with allograft implantation. The first ten years," *Clin. Orthop.*, 69–86 (1983).
4. H. J. Berrey, C. F. Lord, M. C. Gebhardt, and H. J. Mankin, "Fractures of allografts. Frequency, treatment, and end-results," *J. Bone Joint Surg.*, **72A,** 825–833 (1990).
5. F. Lord, M. C. Gebhardt, W. W. Tomford, and H. J. Mankin, "Infection in bone allografts. Incidence, nature, and treatment," *J. Bone Joint Surg.*, **70A,** 369–376 (1988).
6. W. Tomford, J. Thongphasuk, H. J. Mankin, and M. J. Ferraro, "Frozen musculoskeletal allografts. A study of the clinical incidence and causes of infection associated with their use," *J. Bone Joint Surg.*, **72A,** 1137–1143 (1990).
7. Z. Guo, Z. S. Xia, and L. B. Lin, "The mechanical and biological properties of demineralised cortical bone allografts in animals," *J. Bone Joint Surg.*, **73B,** 791–794 (1991).
8. B. Mulliken, J. Glowacki, L. B. Kaban, J. Folkman, and J. E. Murray, "Use of demineralized allogeneic bone implants for the correction of maxillocraniofacial deformities," *Ann. Surg.*, **194,** 366–372 (1981).
9. T. Sonis, L. B. Kaban, and J. Glowacki, "Clinical trial of demineralized bone powder in the treatment of periodontal defects," *J. Oral Med.*, **38,** 117–122 (1983).
10. M. Tuli and A. D. Singh, "The osteoninductive property of decalcified bone matrix. An experimental study," *J. Bone Joint Surg.*, **60B,** 116–123 (1978).
11. J. Upton, M. Boyajian, J. B. Mulliken, and J. Glowacki, "The use of demineralized xenogeneic bone implants to correct phalangeal defects: A case report," *J. Hand Surg.*, **9A,** 388–391 (1984).
12. J. Upton and J. Glowacki, "Hand reconstruction with allograft demineralized bone: Twenty-six implants in twelve patients," *J. Hand Surg.*, **17A,** 704–713 (1992).
13. J. Vandersteenhoven and M. Spector, "Histological investigation of bone induction by demineralized allogeneic bone matrix: A natural biomaterial for osseous reconstruction," *J. Biomed. Mater. Res.*, **17,** 1003–1014 (1983).
14. J. Celeste, J. A. Iannazzi, R. C. Taylor, R. M. Hewick, V. Rosen, E. A. Wange, and J. M. Wozney, "Identification of transforming growth factor beta family members present in bone-inductive protein purified from bovine bone," *Proc. Natl. Acad. Sci. USA*, **87,** 9843–9847 (1990).
15. J. Chen, K. Singh, B. B. Mukherjee, and J. Sodek, "Developmental expression of osteopontin (OPN) mRNA in rat tissues: Evidence for a role for OPN in bone formation and resorption," *Matrix*, **13,** 113–123 (1993).
16. J. Glowacki, C. Rey, M. J. Glimcher, K. A. Cox, and J. Lian, "A role for osteocalcin in osteoclast differentiation," *J. Cell Biochem.*, **45,** 292–302 (1991).
17. E. Ozkaynak, P. N. Schnegelsberg, D. F. Jin, G. M. Clifford, F. D. Warren, E. A. Drier, and H. Oppermann, "Osteogenic protein-2. A new member of the transforming growth factor-beta superfamily expressed early in embyrogenesis," *J. Biol. Chem.*, **267,** 25220–25227 (1992).
18. R. Urist, R. J. DeLange, and G. A. Finerman, "Bone cell differentiation and growth factors," *Science*, **220,** 680–686 (1983).
19. M. R. Urist, "Surface-decalcified allogeneic bone (SDAB) implants. A preliminary report of 10 cases and 25 comparable operations with undecalcified lyophilized bone implants," *Clin. Orthop.*, **56,** 37–50 (1968).
20. I. Kiviranta, M. Tammi, R. Lappalainen, T. Kuusela, and H. J. Helminen, "The rate of calcium extraction during EDTA decalcification from thin bone slices as assessed with atomic absorption spectrophotometry," *Histochemistry*, **68,** 119–127 (1980).
21. J. Makarewicz, L. Harasata, and S. L. Webb, "Kinetics of acid diffusion and demineralization of bone," *J. Photographic Science*, **22,** 148–159 (1980).
22. J. Makarewicz, L. Harasta, and S. L. Webb, "Application of shrinking core kinetics to bone demineralization," *AICHE. SYMP. Series, Vol. 77,* **202,** 141–149 (1981).
23. J. Croome and F. G. Clegg, "Photographic Gelatin," *Focal Press*, London, 1965.
24. M. Eggert and J. P. Germain, "Rapid demineralization in acidic buffers," *Histochemistry*, **59,** 215–224 (1979).
25. O. Levenspiel, *Chemical Reaction Engineering*, Wiley, New York, 1972, pp. 364–365.

Received December 5, 1994
Accepted October 5, 1995